Published in final edited form as:
Nat Nanotechnol. 2010 March ; 5(3): 204–207. doi:10.1038/nnano.2010.26.

Nanostructured films from hierarchical self-assembly of amyloidogenic proteins

Tuomas P. J. Knowles[1], **Tomas W. Oppenheim**[1], **Alexander K. Buell**[1], **Dimitri Y. Chirgadze**[2], and **Mark E. Welland**[1,*]

[1]Nanoscience Centre, J J Thomson Avenue, University of Cambridge, Cambridge CB3 0FF, UK

[2]Department of Biochemistry, Tennis Court Road, University of Cambridge, Cambridge CB2 1GA, UK

Abstract

In nature, sophisticated functional materials are created through hierarchical self-assembly of simple nanoscale motifs[1–4]. In the laboratory, much progress has been made in the controlled assembly of molecules into one-[5–7], two-[6,8,9] and three-dimensional[10] artificial nanostructures, but bridging from the nanoscale to the macroscale to create useful macroscopic materials remains a challenge. Here we show a scalable self-assembly approach to making free-standing films from amyloid protein fibrils. The films were well ordered and highly rigid, with a Young's modulus of up to 5–7 GPa, which is comparable to the highest values for proteinaceous materials found in nature. We show that the self-organizing protein scaffolds can align otherwise unstructured components (such as fluorophores) within the macroscopic films. Multiscale self-assembly that relies on highly specific biomolecular interactions is an attractive path for realizing new multifunctional materials built from the bottom up.

We designed a strategy to take advantage of the propensity of amyloidogenic protein molecules[1,11] to create highly specific, non-covalent contacts to fabricate macroscopic materials with controlled nanostructure (Fig. 1a–c). Amyloidogenic proteins are polypeptide molecules capable of self-assembly into β-sheet rich linear aggregates; such structures[12,13] were first discovered in association with a range of disease states, but are now known to be of more general significance. Indeed, it has become apparent that many proteins that do not possess structural similarities or sequence homology with disease-related proteins are also capable of undergoing such fibrillar self-assembly[14]. Furthermore, amyloid or amyloid-like structures have been discovered in functional roles[11,15–17] in nature in contexts as diverse as epigenetic information transfer, catalytic scaffolds and bacterial coatings, findings consistent with the idea that the amyloid cross-β fold is accessible to a wide variety of protein

*Correspondence and requests for materials should be addressed to M.E.W. mew10@cam.ac.uk.

Author contributions

T.P.J.K., T.W.O., A.K.B. and D.Y.C. performed the experiments. T.P.J.K., T.W.O., D.Y.C. and M.E.W. analysed the data. T.P.J.K., A.K.B. and M.E.W. co-wrote the paper. All authors discussed the results and commented on the manuscript.

The authors declare no competing financial interests.

Supplementary information accompanies this paper at www.nature.com/naturenanotechnology.

Europe PMC Funders Author Manuscripts

molecules and represents a generic characteristic of polypeptide chains[11,13]. Hierarchical self-assembly has been shown to be a powerful tool for the creation of nanostructured materials[18,19]. We use fibrillar polypeptide self-assembly in a two-step process. In a first step, protein molecules are assembled into elongated fibrils (Fig. 1b) under conditions where the formation of intermolecular interactions is favoured over intramolecular ones (see Methods). The resulting nanofibrils have been shown to be highly stable and rigid[5,20]. Furthermore, these densely hydrogen-bonded structures can be formed from a range of different peptides and proteins[1,11,21]. In a second step, the fibrils are cast into thin films (Fig. 1c). We show (Fig. 1d and Fig. 2a–c) that, during the casting process, the fibrils align in the film plane (Fig. 2c) and that in the presence of plasticizing molecules the fibrils stack with nematic order (Fig. 1d and Fig. 2b), resulting in materials that have a hierarchy of length scales: nanometre ordering within the fibrils and micrometre-scale ordering in the stacking of the fibrils. The nematic order on macroscopic scales in the nanostructured films leads to interaction with visible light and can be observed clearly by polarization microscopy. Figure 1d shows a single domain film, which transmits light uniformly when positioned at an angle of 45° between crossed polarizers, and is opaque when parallel to one of the polarizers. Our films have many similarities with films produced from monomeric proteins such as those studied, for example, for applications as edible packaging materials[22]. The two-step assembly process, however, enables materials to be produced that possess a well-defined hierarchy of length scales. Using this method, films with lateral dimensions up to the centimetre scale could be routinely fabricated, a practical size defined essentially by the brittleness of the films as well as by their low thickness, which makes the convenient handling of free-standing films of significantly larger dimensions more challenging.

Characterization of the films by X-ray diffraction measurements (Fig. 2a–c) reveals that they possess a high level of order on the nano- (Fig. 2a–c) and micrometre (Fig. 2b,c) scales. Insight into the structure of the material can be obtained from examining the characteristic distances and orientations of the two major length scales present. The individual β-strands composing the nanofibrils are separated by 4.8 Å along the fibril direction, and the sheets composed of arrays of strands associate laterally to form parallel assemblies, giving rise to a characteristic distance of approximately 12 Å in the direction perpendicular to the strand repeat[23]. When the nanostructures are cast from the hydrogel (see Methods) into the films, the long axes of the fibrils are aligned in the film plane as observed by X-ray scattering (Fig. 2c). These results also show that the casting and drying process does not degrade the highly regular atomic-level core structure[23,24] of the fibrils. If plasticizing molecules such as small molecular-weight polyethylene glycol are added to the suspension of nanostructures before the casting process (see Methods), further ordering can be observed and the fibrils adopt nematic order in the solid phase (Fig. 2b). Liquid-crystalline behaviour of elongated biomolecular assemblies in solution is well known[25,26], and the presence of a plasticizer could enable this orientational order to be preserved in the solid phase through inter-fibril lubrication, competition for inter-fibril interactions, or by enhancing the tendency for orientational ordering as a result of depletion interactions.

To characterize the mechanical properties of the protein films, we performed flexural testing in three-point (Fig. 3) and cantilever geometries (Supplementary Fig. S1). In the three-point geometry (Fig. 3a) both ends of a film were supported and an oscillating load was applied to

the suspended centre section. The results in Fig. 3b reveal that the elastic moduli of the films ranges from 5.2 to 6.2 GPa for lysozyme films and from 6.7 to 7.2 GPa for β-lactoglobulin, and are therefore only lowered by a small fraction when compared in Fig. 3c to the mechanical properties of the individual structures (Young's modulus, 2–19 GPa)[5,20,27]. In particular, the films have a Young's modulus that is similar to that of the most rigid proteinaceous materials found in nature, such as keratin and collagen (Fig. 3c). The high level of transmission of nanoscale mechanical properties to macroscopic films is remarkable in view of the fact that the analogous films generated from high-performance carbon-based nanomaterials, such as 'bucky paper', formed from carbon nanotubes, show an elastic modulus and tensile strength of the bulk material that are typically several orders of magnitude lower than the corresponding characteristics of the individual nanostructures[28]. This lowering of the mechanical properties when the size of the material is scaled up is a fundamental limitation for the production of high-performance macroscopic forms of nanomaterials and has been ascribed to the difficulty in establishing robust contacts between adjacent nanotubes. Protein nanofibrils, however, have an outer surface rich in functional groups that could help to ensure efficient connectivity between the structures through hydrophobic packing and the large surface area for van der Waals contacts.

Finally, we illustrate the power of self-assembling protein scaffolds in controlling the organization of objects such as fluorophores that, on their own, do not generally have a strong tendency to generate complex structures. When the fibrils adopt nematic order in the film state, they can direct the alignment of the dipole moments of attached fluorophores in a single direction, thereby producing a material that emits polarized light under optical excitation. We chose as a fluorophore the planar aromatic dye Thioflavin T, which can attach to β-sheet-rich structures with the orientation of the emission dipole parallel to the sheet length, which coincides with the long axis of the fibril[29]. The fluorescence of the molecule is maintained in the casting and drying process. The optical characteristics of the resulting material were tested by exciting the film with *s*-polarized light. The emitted light, collected in a direction perpendicular to the excitation beam, was also transmitted through a polarization filter, with the same orientation as the excitation wave, and the intensity at the emission wavelength was recorded (see Methods). When the film was rotated in the plane through 360° the intensity of the emission varied significantly (Fig. 4). Emission maxima, separated by 180°, correspond to the dipole axis being parallel to the filter orientation, and the minima, separated from the maxima by 90° (Fig. 3), corresponding to perpendicular relative orientation, thereby demonstrating that the molecular-level alignment of the fluorophores could be achieved using the organized proteinaceous scaffold.

It is interesting to note that, although structures very similar to the amyloid-like fibrils we have used here to fabricate nanostructured biofilms are found in deposits associated with pathological conditions such as Alzheimer's and Parkinson's diseases[1,12], there are cases where biology has used the amyloid-structure as a basis for functional materials[15–17]. One example of such a natural application is protein-based functional microbial coatings[16]; it is interesting to speculate that the very characteristics that are achieved in the artificial films of the present study, such as convenient multiscale self-assembly and mechanical rigidity, also underlie the natural function of amyloid materials as coatings in microbiology.

Europe PMC Funders Author Manuscripts

In this paper we have used the high specificity of biomolecular interactions to fabricate nanostructured films through a multiscale self-assembly process. Owing to the combination of accurate self-assembly and chemical versatility with regard to possibilities for surface functionalization, such protein-based nanostructured films represent an attractive path towards realizing new multifunctional materials built from the bottom up.

Methods

Amyloid film preparation

Hen egg white lysozyme (Sigma Aldrich) was incubated as a 3% w/w solution in aqueous 10 mM hydrochloric acid at 65 °C for 14 days to induce self-assembly into nanofibrils. The fibrillar content was improved in a second step by adding 5% v/v of this pre-formed fibril suspension as seed material at the beginning of the subsequent polymerization reaction, which was carried out for 7 days at 65 °C. At the end of the fibril growth step, plasticizers (up to 0.8% v/v PEG 400 or glycerol, Sigma Aldrich) were added to the hydrogel. Films were then cast by transferring 1 ml of the nanofibril containing hydrogel onto a flat polytetrafluoroethylene film; the solvent and the volatile acid were left to evaporate for 24 h and the resulting protein films could be removed with tweezers. Films containing plasticizers could be cut to a desired shape using a razor blade, whereas films from pure protein fibrils were more brittle and could be broken to size with the use of tweezers. Strong nematic ordering was observed in the presence of PEG 400 (Fig. 2b), in contrast to films cast without plasticizer (Fig. 2a). The preparation of films from β-lactoglobulin followed a similar protocol: bovine β-lactoglobulin (Sigma Aldrich) was incubated at a concentration of 1% w/w in 10 mM HCl at 60 °C for 48 h, resulting in the formation of a fibril hydrogel of lower viscosity than in the case of lysozyme. Films were cast as for lysozyme. Using this method, free-standing films with thicknesses varying from 15 μm to 100 mm and lateral dimensions in the centimetre range were produced.

Films functionalized with fluorophores

A filtered solution (pore size, 220 nm) of Thioflavin T (Sigma Aldrich) was prepared with a concentration of 10 mg ml^{-1} in water, and 1 μl was added to 1 ml of the lysozyme nanofibril hydrogel containing PEG 400, prepared as described above, and mixed using a vortex mixer for 30 s. The fluorescence of the films was measured using a Cary Eclipse Fluorimeter equipped with polarizers. A 10 mm × 10 mm piece of the film was fixed between two round quartz plates. The active region where emission was measured was limited to a circle by using a mask attached to the top quartz plate to ensure that the surface over which the signal was recorded remained constant when the sample was rotated. The sample was then rotated in the plane through 360°, in increments of 45°, and an emission spectrum was measured from 460 to 600 nm and the value at the maximum, 482 nm, was recorded. The excitation wavelength used was 440 nm. Excitation and emission directions were in the horizontal plane at right angles, and polarizers with vertical orientation were used for both the emission and excitation paths. The azimuthal angle of the film plane was chosen such that emission and excitation were both from one side of the film.

X-ray diffraction studies

X-ray diffraction studies were performed at the crystallographic diffraction data collection facility, Department of Biochemistry, University of Cambridge. X-rays with a wavelength of 1.54 Å were produced by a rotating copper anode generator RU-H3R (Rigaku-MSC), and collimated and focused by Osmic Max-ux optics. Images were acquired on a Raxis-IV++ image plate (Rigaku-MSC). Data acquisition times were between 5 and 20 min.

Mechanical measurements

Measurements were performed in a three-point bending geometry on a TA-Instruments Q800 DMA set-up using lysozyme and β-lactoglobulin films fabricated without plasticizers. The storage modulus E was computed from the measured stiffness k_s as $E = k_s L^3/(48I)$, where $I = wh^3/12$ is the cross-sectional moment of inertia and w, h and L denote the width, thickness and length of the suspended film[30]. The oscillation amplitude was 5 μm and the oscillation frequency varied between 1 and 10 Hz. The thickness of the films was measured by scanning electron microscopy (Fig. 1c): fractured films were sputter-coated with platinum and imaged using a LEO 1530 VP microscope. The lateral dimensions of the films were measured using micrometers.

Supplementary Material

Refer to Web version on PubMed Central for supplementary material.

Acknowledgements

The authors acknowledge support from Nokia Research Cambridge, the UK Engineering and Physical Sciences Research Council (EPSRC), the Interdisciplinary Research Council (IRC) in Nanotechnology, St John's College, Cambridge, and the Wellcome Trust. We thank C. Dobson, E. Eiser, M. Haddow and C. Meier for valuable discussions, and A. Rayment and I. Ganney for assistance with the mechanical measurements.

References

1. Dobson CM. Protein folding and misfolding. Nature. 2003; 426:884–890. [PubMed: 14685248]
2. Buehler MJ, Ackbarow T. Nanomechanical strength mechanisms of hierarchical biological materials and tissues. Comput. Methods Biomech. Biomed. Eng. 2008; 11:595–607. [PubMed: 18803059]
3. Buehler MJ, Yung YC. Deformation and failure of protein materials in physiologically extreme conditions and disease. Nature Mater. 2009; 8:175–188. [PubMed: 19229265]
4. Whitesides GM, Grzybowski B. Self-assembly at all scales. Science. 2002; 295:2418–2421. [PubMed: 11923529]
5. Kol N, et al. Self-assembled peptide nanotubes are uniquely rigid bioinspired supramolecular structures. Nano Lett. 2005; 5:1343–1346. [PubMed: 16178235]
6. Zhang S. Fabrication of novel biomaterials through molecular self-assembly. Nature Biotechnol. 2003; 21:1171–1178. [PubMed: 14520402]
7. Mao C, et al. Virus-based toolkit for the directed synthesis of magnetic and semiconducting nanowires. Science. 2004; 303:213–217. [PubMed: 14716009]
8. Rothemund PWK. Folding DNA to create nanoscale shapes and patterns. Nature. 2006; 440:297–302. [PubMed: 16541064]
9. Zhang S, Holmes T, Lockshin C, Rich A. Spontaneous assembly of a self-complementary oligopeptide to form a stable macroscopic membrane. Proc. Natl Acad. Sci. USA. 1993; 90:3334–3338. [PubMed: 7682699]

10. Goodman RP, et al. Rapid chiral assembly of rigid DNA building blocks for molecular nanofabrication. Science. 2005; 310:1661–1665. [PubMed: 16339440]
11. Chiti F, Dobson CM. Protein misfolding, functional amyloid, and human disease. Annu. Rev. Biochem. 2006; 75:333–366. [PubMed: 16756495]
12. Kelly JW. Towards an understanding of amyloidogenesis. Nature Struct. Biol. 2002; 9:323–325. [PubMed: 11976724]
13. Dobson CM. Protein misfolding, evolution and disease. Trends Biochem. Sci. 1999; 24:329–332. [PubMed: 10470028]
14. Fändrich M, Fletcher MA, Dobson CM. Amyloid fibrils from myoglobin. Nature. 2001; 410:165–166. [PubMed: 11242064]
15. Fowler DM, Koulov AV, Balch WE, Kelly JW. Functional amyloid—from bacteria to humans. Trends Biochem. Sci. 2007; 32:217–224. [PubMed: 17412596]
16. Chapman MR, et al. Role of *Escherichia coli* curli operons in directing amyloid fiber formation. Science. 2002; 295:851–855. [PubMed: 11823641]
17. Maji SK, et al. Functional amyloids as natural storage of peptide hormones in pituitary secretory granules. Science. 2009; 325:328–332. [PubMed: 19541956]
18. Huang Y, Duan X, Wei Q, Lieber CM. Directed assembly of one-dimensional nanostructures into functional networks. Science. 2001; 291:630–633. [PubMed: 11158671]
19. Ikkala O, ten Brinke G. Functional materials based on self-assembly of polymeric supramolecules. Science. 2002; 295:2407–2409. [PubMed: 11923526]
20. Knowles TP, et al. Role of intermolecular forces in defining material properties of protein nanofibrils. Science. 2007; 318:1900–1903. [PubMed: 18096801]
21. Reches M, Gazit E. Controlled patterning of aligned self-assembled peptide nanotubes. Nature Nanotech. 2006; 1:195–200. [PubMed: 18654186]
22. Gennadios, A., editor. Protein Based Films and Coatings. CRC Press; 2002.
23. Sawaya MR, et al. Atomic structures of amyloid cross-beta spines reveal varied steric zippers. Nature. 2007; 447:453–457. [PubMed: 17468747]
24. Jaroniec CP, et al. High resolution molecular structure of a peptide in an amyloid fibril determined by magic angle spinning NMR spectroscopy. Proc. Natl Acad. Sci. USA. 2004; 101:711–716. [PubMed: 14715898]
25. Donald, AM.; Windle, AH.; Hanna, S. Liquid Crystalline Polymers. 2nd edn. Cambridge Univ. Press; 2006.
26. Corrigan AM, Müller C, Krebs MRH. The formation of nematic liquid crystal phases by hen lysozyme amyloid fibrils. J. Am. Chem. Soc. 2006; 129:14740–14741. [PubMed: 17105248]
27. Smith JF, Knowles TPJ, Dobson CM, Macphee CE, Welland ME. Characterization of the nanoscale properties of individual amyloid fibrils. Proc. Natl Acad. Sci. USA. 2006; 103:15806–15811. [PubMed: 17038504]
28. Baughman RH, Zakhidov AA, de Heer WA. Carbon nanotubes—the route toward applications. Science. 2002; 297:787–792. [PubMed: 12161643]
29. Krebs MRH, Bromley EHC, Donald AM. The binding of thioflavin-T to amyloid fibrils: localisation and implications. J. Struct. Biol. 2005; 149:30–37. [PubMed: 15629655]
30. Kosevich, AM.; Lifshitz, EM.; Landau, LD.; Pitaevskii, LP. Theory of Elasticity. Butterworth-Heinemann; 1986.

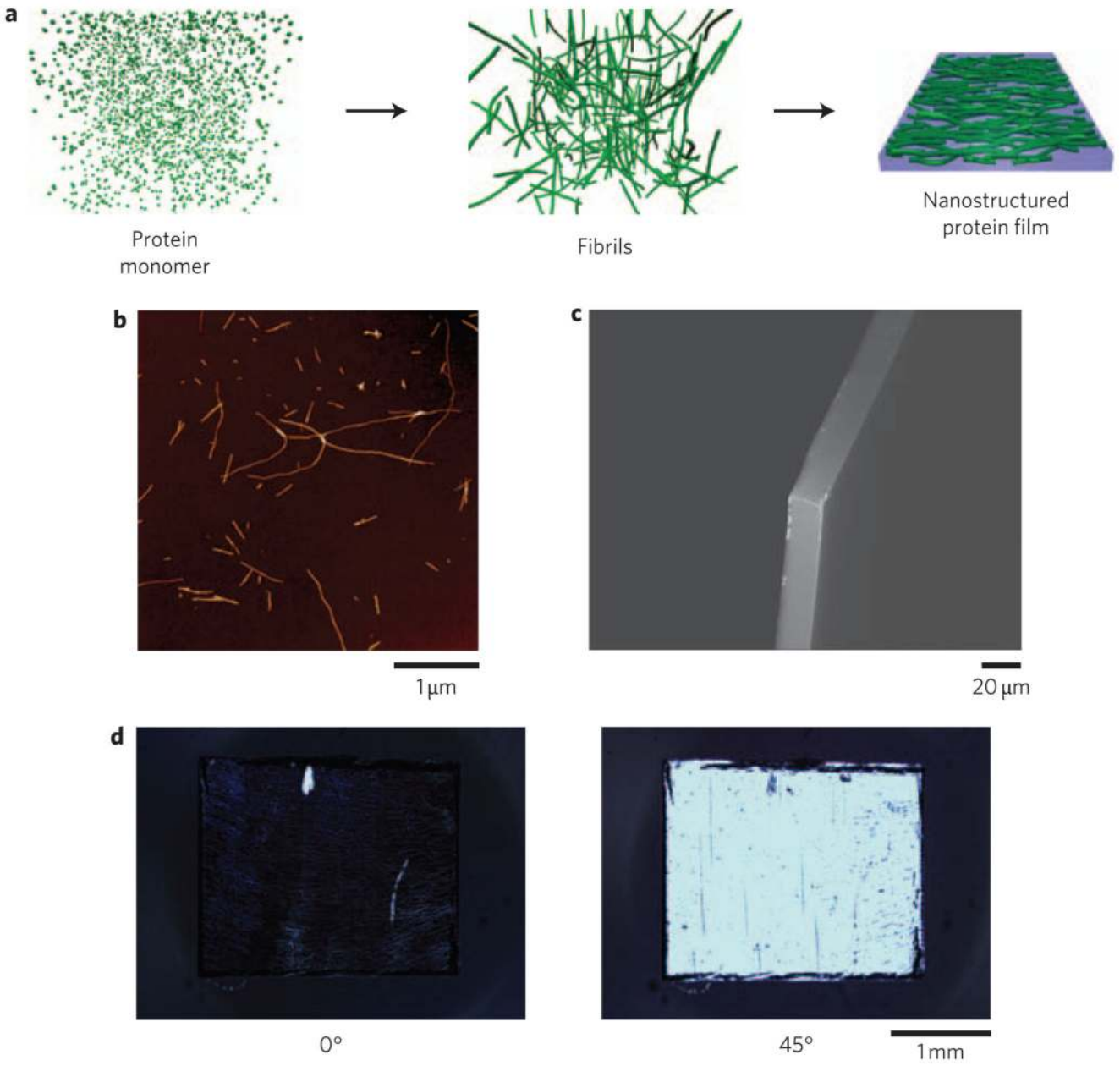

Figure 1. Fabrication of nanostructured films through multiscale hierarchical self-assembly

a, Protein molecules are first assembled into amyloid fibrils, which are then stacked into films. **b**, Atomic force micrograph of the component lysozyme fibrils. **c**, Scanning electron micrograph of the resulting free-standing protein film. **d**, Optical images of plasticizer containing lysozyme amyloid films under crossed polarizers show low transmission through the protein film when the objective polarizer is parallel to the fibril alignment in the film (left) and maximal transmission at an angle of 45° (right).

Europe PMC Funders Author Manuscripts

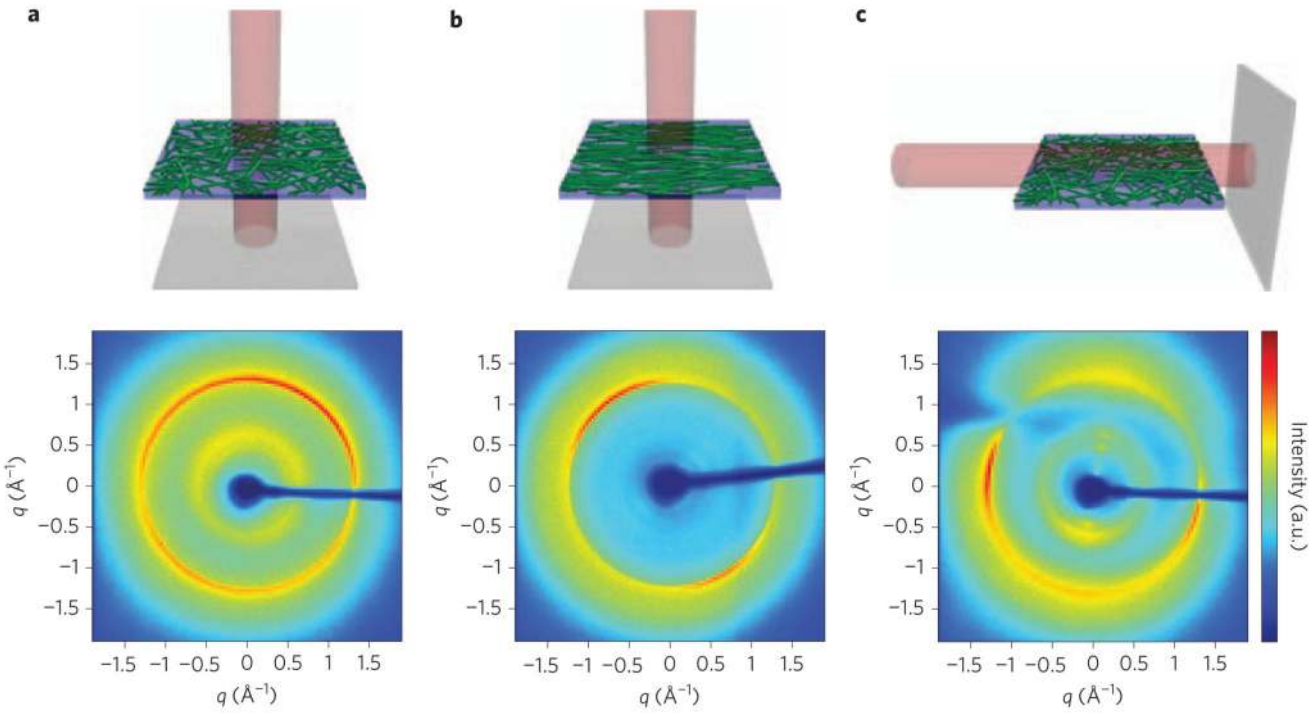

Figure 2. Characterization of nanostructured protein films by X-ray diffraction studies

a–c, Top row shows the exposure geometry and bottom row shows the respective X-ray data. Film without (**a**) and with (**b**) plasticizer, illuminated from the top, showing an isotropic orientation of the characteristic inter-sheet and inter-strand repeats (**a**) and orientational order, with the inter-sheet and inter-strand orientations being perpendicular to each other as required by the fibril geometry (**b**). **c**, Same film as in **a**, illuminated from the side, demonstrating the alignment of the fibrils in the film plane as described in the main text.

Europe PMC Funders Author Manuscripts

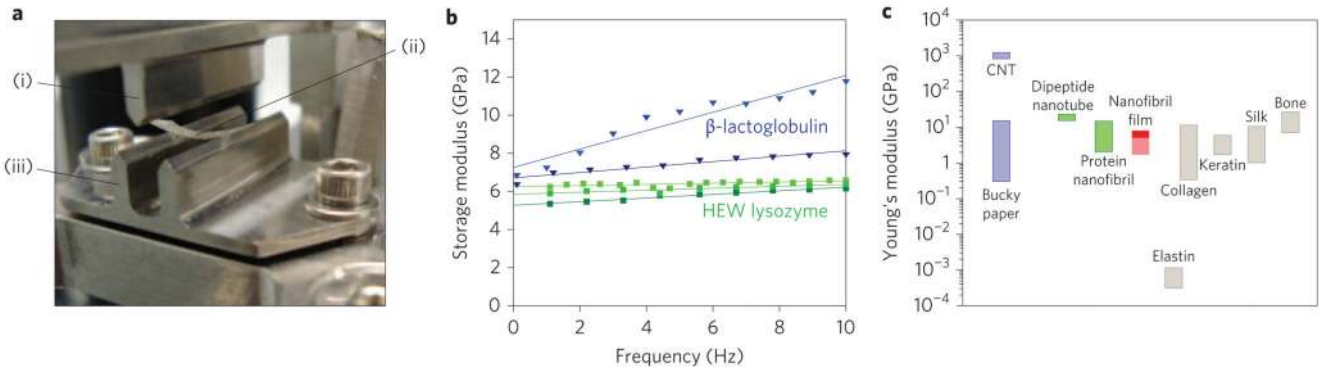

Figure 3. Mechanical testing of nanostructured protein films in a three-point bending geometry

a, An oscillating load is applied (i) to the centre section (ii) of the film suspended between the supporting clamps (iii). **b**, Graph shows storage modulus as a function of frequency *f* for different film samples from lysozyme (green squares, three individual films) and β-lactoglobulin (blue triangles, two individual films) and the extrapolation $f \rightarrow 0$ to give the Young's modulus. **c**, Comparison of Young's moduli of different materials shows that the artificial nanostructured protein films have moduli (dark red rectangle: three-point bending geometry, data from Fig. 3b; light red rectangle: cantilever geometry, data from Supplementary Information) in the upper range for biomaterials.

Europe PMC Funders Author Manuscripts

Europe PMC Funders Author Manuscripts

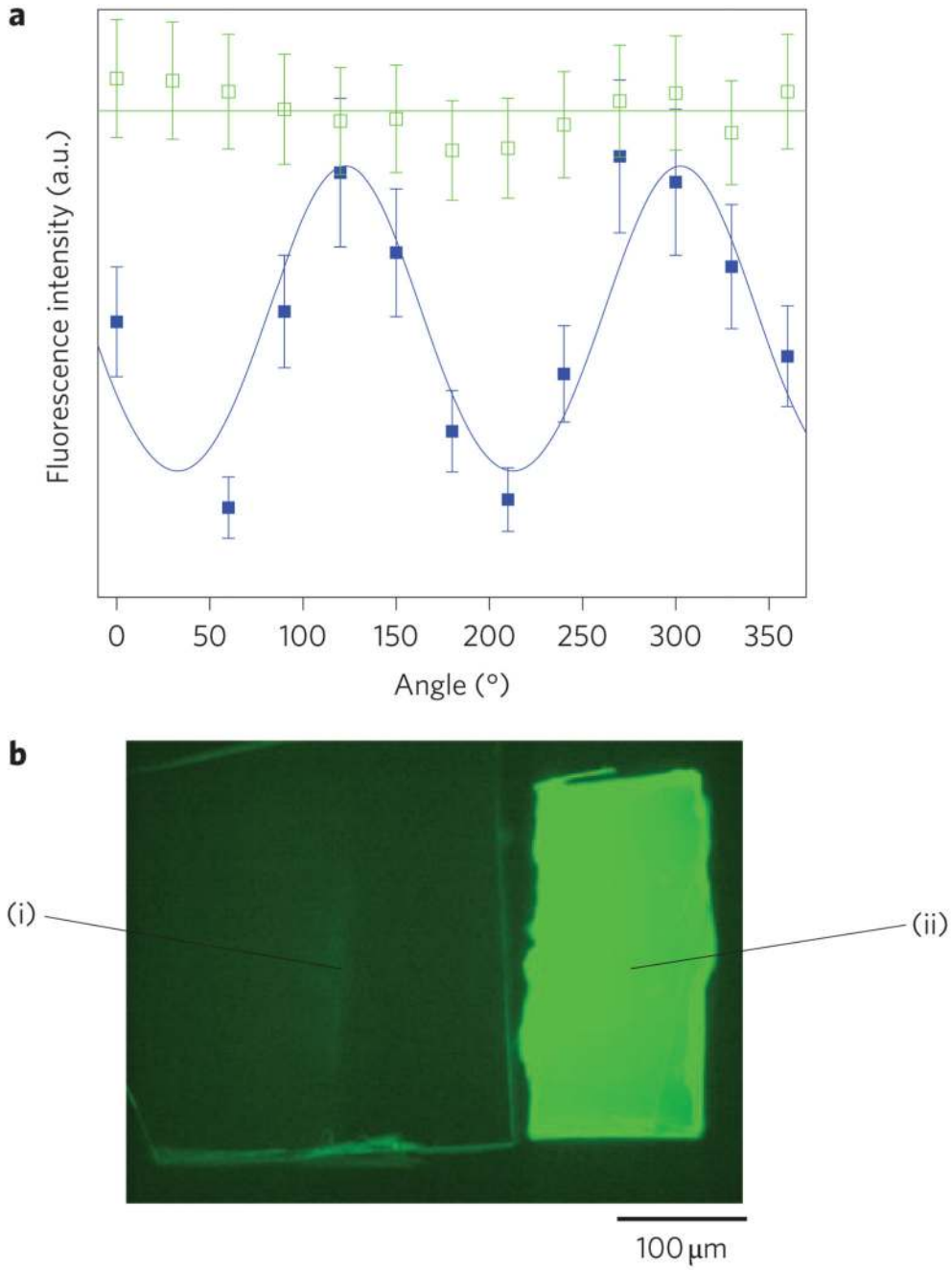

Figure 4. Nanoscale alignment of fluorophores through self-organizing protein scaffolds

a, Plot showing the intensity of the emission of light from nanostructured films containing aligned fluorophores. The emitted light was transmitted through a polarizing filter with a fixed orientation, and the orientation of the film was changed through 360° by rotating the sample in the plane (filled blue squares); as a guide to the eye, a fit to the function $[\text{const} + A \sin(\alpha + \phi)^2]^2$ is shown in blue, where const is an offset that includes contributions from the emission of the unoriented population of fluorophores, A represents an amplitude of the excitation wave and ϕ a shift between the measured film angle α and the true direction of

fibril alignment. The green open squares represent data from an equivalent measurement without the presence of the polarizers. A constant offset was subtracted from the control data intensity to facilitate comparison. The relative error on the fluorescence intensity was assumed to be constant and was estimated from repeated measurements at a fixed angle. **b**, Fluorescence microscopy image of a non-functionalized (i) and functionalized (ii) fibril film.

Europe PMC Funders Author Manuscripts